Intermittent Granular Dynamics at a Seismogenic Plate Boundary

Yasmine Meroz[1,*] and Brendan J. Meade[2]
[1]John A. Paulson School of Engineering and Applied Sciences, Harvard University, Cambridge, Massachusetts 02138, USA
[2]Department of Earth and Planetary Sciences, Harvard University, Cambridge, Massachusetts 02138, USA
(Received 23 April 2017; published 26 September 2017)

Earthquakes at seismogenic plate boundaries are a response to the differential motions of tectonic blocks embedded within a geometrically complex network of branching and coalescing faults. Elastic strain is accumulated at a slow strain rate on the order of 10^{-15} s^{-1}, and released intermittently at intervals >100 yr, in the form of rapid (seconds to minutes) coseismic ruptures. The development of macroscopic models of quasistatic planar tectonic dynamics at these plate boundaries has remained challenging due to uncertainty with regard to the spatial and kinematic complexity of fault system behaviors. The characteristic length scale of kinematically distinct tectonic structures is particularly poorly constrained. Here, we analyze fluctuations in Global Positioning System observations of interseismic motion from the southern California plate boundary, identifying heavy-tailed scaling behavior. Namely, we show that, consistent with findings for slowly sheared granular media, the distribution of velocity fluctuations deviates from a Gaussian, exhibiting broad tails, and the correlation function decays as a stretched exponential. This suggests that the plate boundary can be understood as a densely packed granular medium, predicting a characteristic tectonic length scale of 91 ± 20 km, here representing the characteristic size of tectonic blocks in the southern California fault network, and relating the characteristic duration and recurrence interval of earthquakes, with the observed sheared strain rate, and the nanosecond value for the crack tip evolution time scale. Within a granular description, fault and blocks systems may rapidly rearrange the distribution of forces within them, driving a mixture of transient and intermittent fault slip behaviors over tectonic time scales.

DOI: 10.1103/PhysRevLett.119.138501

Fault slip at seismogenic plate boundaries is rarely continuous, instead occurring intermittently during short duration earthquakes which last from seconds [1] to minutes [2], during which fault slip may reach up to 50 m [3]. Throughout the interseismic interval between large earthquakes, plate boundaries are not dormant but instead slowly accumulate the elastic strain that will be released in future earthquakes [4], while the faults themselves are frictionally locked. In addition to this temporally bimodal behavior, fault slip at plate boundaries is not localized along a single fault but rather spread across fault systems where faults are bounded by tectonic blocks to form anastomosing fault systems [5–7].

Dynamic models of activity at seismogenic plate boundaries have generally focused on the physics within narrow (<1 m) individual fault shear zones [8–12]. However, while large faults (e.g., the San Andreas Fault in California) accommodate the majority of deformation between two plates (e.g., the Pacific and North American plates), they are embedded within a geometrically complex network of branching and coalescing faults [5,13], as can be appreciated in Fig. 1, and the interactive map in Ref. [14].

Here, we investigate the macroscopic dynamics of planar tectonics within such fault and block systems occurring on scales >100 km, while considering the suggestion [16] that sheared granular systems may provide an analog. Both systems exhibit intermittent dynamics manifested in a gradual increase in elastic energy released by a precipitous event; in slowly sheared granular media, these are rearrangement events of single granules, while in seismogenic plate boundaries, these are earthquakes. Moreover, in both systems the motion at the boundaries is defined and results from the differential motion of the granules or tectonic blocks adjoining a potential slip surface. Here, we consider the extent to which scaling laws derived from numerical simulations of slowly sheared 2D deformable granular systems (foam) [17–19] may describe earthquake cycle activity at tectonic plate boundaries, including spatial variabilities of nominally interseismic Global Positioning System (GPS) velocities across the Pacific–North America plate boundary in California, as well as characteristic earthquake cycle time scales.

We consider 1106 nominally interseismic GPS velocity observations, recorded over a period of ~10 yr on average, in the area sheared between the Pacific and North American plates in California [15]. The area is defined as running from the Pacific plate at the bottom, where we define $y = 0$, to the North American plate at the top, where $y = L = 565$ km, while the x axis runs along $0 < x < 1200$ km, approximately parallel to the San Andreas Fault. The velocities $\mathbf{v}_i$ at each GPS reading i are calculated relative to the North American plate and are

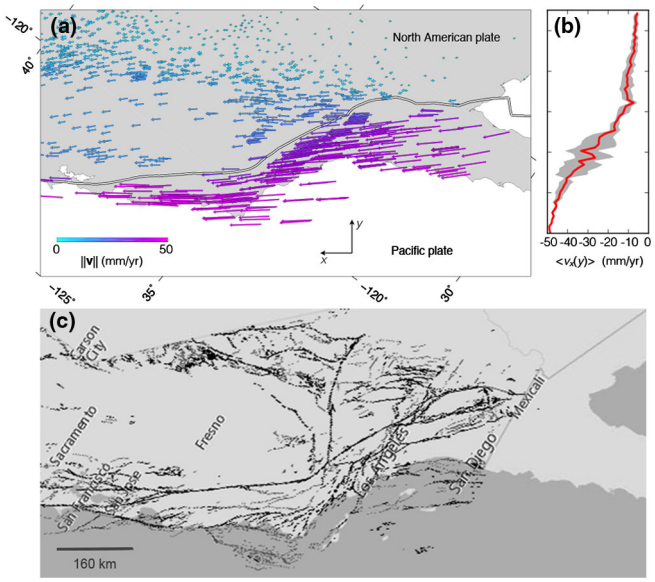

FIG. 1. (a) Vector field of 1106 interseismic GPS velocities from across the Pacific–North American plate boundary in California [15], where magnitude is given by color and size. The x axis is approximately parallel to the trace of the San Andreas Fault shown here, while the y axis runs across $L = 565$ km from the Pacific to the North American plate. (b) Average velocity profile as a function of y position in (a). Standard deviation in grey. (c) The full fault system: a geometrically complex network of branching and coalescing faults which accommodates the deformation between the Pacific and North American plates [14], spread across > 100 km.

shown in Fig. 1(a), represented by a vector field. Relative velocities exhibit a clear trend, with lower absolute values closer to the North American plate (here considered fixed), and increasing values closer to the moving Pacific plate, with a maximum of ~ 50 mm/year. We calculate the average velocity profile along the y axis, $\langle \mathbf{v}(y) \rangle$, by discretizing the y axis into $N = 65$ bins, with $dy = 8.7$ km. The discretized velocity profile is then calculated as the average velocity of readings within the same bin. For simplicity, in what follows we will adopt the continuous notation $\langle \mathbf{v}(y) \rangle$. The average velocity profile is shown in Fig. 1(b), exhibiting nonlinearity, i.e., shear bands, as also observed experimentally in different sheared granular systems [20]. The shear strain rate, defined as the relative velocity of the two plates divided by the distance between them, i.e., $\dot{\epsilon} = (\langle v_x(L) \rangle - \langle v_x(0) \rangle)/L$, yields $\dot{\epsilon} = 7.66 \times 10^{-8}$ (1/yr). We define the fluctuation of the velocity of a reading from the average velocity profile as

$$\delta \mathbf{v}_i = \mathbf{v}_i - \langle \mathbf{v}(y_i) \rangle, \tag{1}$$

where $\mathbf{v}_i$ is the velocity of the reading i, and $\langle \mathbf{v}(y_i) \rangle$ is the average velocity at position y_i associated with the reading i. To characterize the kinematics of the system as manifested by the velocity fluctuations, we calculate the distribution of velocity fluctuations of the GPS readings $P(\delta \mathbf{v})$, and the equal-time spatial correlation function,

$$C(r) = \frac{\langle \delta \mathbf{v}(r) \cdot \delta \mathbf{v}(0) \rangle}{\langle \delta \mathbf{v}^2 \rangle}. \tag{2}$$

We consider the analogy between the intermittent earthquake events, which release energy accumulated due to the shearing of tectonic plates along a fault, and the intermittent rearrangement events in sheared 2D granular systems, and we compare our results to those of numerical simulations of a slowly sheared 2D deformable granular medium (foam) [17]. For slow shearing rates, the distribution of velocity fluctuations has been found to deviate from a Gaussian (expected for fluidlike flow at high shearing rates), and spatial correlations follow a stretched exponential (deviating from the exponential expected for fluid behavior).

The distribution of velocity fluctuations of the GPS observations in the x and y directions, $P(\delta v_x)$ and $P(\delta v_y)$, are plotted in Fig. 2, and their fit to a Gaussian distribution is added for comparison. The distributions deviate significantly from a Gaussian distribution, exhibiting heavy tails. This is further confirmed by calculating the non-Gaussian parameter (NGP) [21] for different moment ratios:

$$\alpha_n(x) = \frac{\langle x^{2n} \rangle}{C_n \langle x^2 \rangle^n} - 1, \tag{3}$$

where C_n is a known constant. By definition, α_n equals zero for Gaussian distributions. Here, we calculate α_2 and α_3, where, in 2D, $C_2 = 3$ and $C_3 = 15$. The NGP calculated for the fluctuations in the x direction yield $\alpha_2 = 0.25$ and

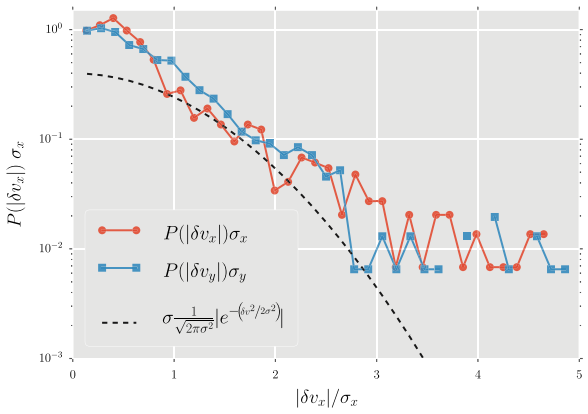

FIG. 2. Plot of the distributions of the velocity fluctuations $P(\Delta v_x)$ (the red circles) and $P(\Delta v_y)$ (the blue squares). We collapse the distributions by plotting them multiplied by the standard deviation σ_x or σ_y accordingly, as a function of the absolute value of velocity fluctuations rescaled by the standard deviation [17]. We use a semilogarithmic scale. A Gaussian distribution (the dashed line) is plotted for comparison, highlighting the heavy tails of the distributions, which clearly deviate from a Gaussian at high velocities.

$\alpha_3 = 0.47$, and in the y direction $\alpha_2 = 0.62$ and $\alpha_3 = 2.18$. For comparison, we calculate these values for a numerically generated Gaussian distribution with an identical population size, yielding $\alpha_2 = -0.05$ and $\alpha_3 = -0.18$, highlighting that the NGP values calculated for the original distributions clearly indicate non-Gaussianity.

We note that a part of the San Andreas Fault deviates from the horizontal orientation of the plates within the area analyzed here, as depicted in Fig. 1(a). In order to rule out the possibility that the broad distribution of velocity fluctuations may be an artifact due to this slope, we carry out the analysis for the left third of the plate boundary, where the fault is relatively horizontal [details in the Supplemental Material (SM) [22]]. We find that the heavy tails are even more pronounced (see Fig. S2 of the SM [22]), showing the independence of our results on the geometric form of the San Andreas Fault. Moreover, substantial fluctuations are not limited to the San Andreas Fault, but rather are exhibited in an area of ~100 km across the fault (see Fig. S1 of the SM [22]).

To calculate the spatial distribution of velocity fluctuations, we limit ourselves to ~200 km around the fault (roughly 100 km $< y <$ 300 km), thus avoiding recordings associated with the plates themselves which would mask the relevant correlation. In Fig. 3 we plot the calculated spatial correlation of velocities fluctuations according to Eq. (2). We fit this to the general form of a stretched exponential:

$$F(r) = e^{-(r/\xi)^{\beta}}, \tag{4}$$

yielding the values $\beta = 0.75$ and $\xi = 92$ km, with $R^2 = 0.92$ of the least squares fit. We note that a stretched exponential can be approximated with an exponential for short scales; however, the two diverge significantly at long scales. This deviation is evident in the inset of Fig. 3, where $C(r)$ is plotted on a semilogarithmic scale, with the exponential function $e^{-(r/\xi)}$ plotted for reference. In the SM [22] we show that this deviation is not the result of noisy statistics, and moreover that the value of ξ is robust to different binning sizes. Simulations for 2D sheared foam at low shearing rates [17] exhibit values of $\beta < 1$, deviating from a regular exponential behavior with $\beta = 1$, and ξ is found to be associated with the average granule or bubble size.

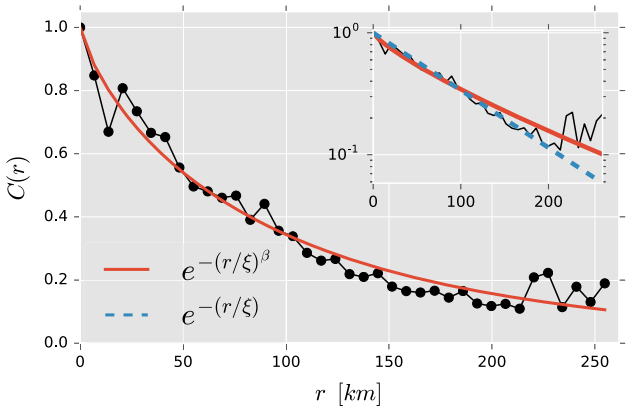

FIG. 3. Equal-time spatial correlation function of velocities fluctuations calculated as in Eq. (2), $C(r) = \langle \delta\mathbf{v}(r) \cdot \delta\mathbf{v}(0)\rangle / \langle \delta\mathbf{v}^2\rangle$ (the dotted line), and fit to the stretched exponential function in Eq. (4), $e^{-(r/\xi)^{\beta}}$ (the solid line). The fit yields $\beta = 0.75$ and $\xi = 92$ km, with $R^2 = 0.92$ of the least squares fit. (Inset) Plot of the correlation function on a semilog scale, with an exponential (the dashed blue line) shown for comparison.

In this Letter we investigate macroscopic planar tectonic dynamics across a geometrically complex network of faults and blocks accommodating the deformation between the North American and Pacific plates in California on scales > 100 km. Here, we consider the similarity between fault block systems and the intermittent dynamics of granular systems sheared at low shearing rates, both of which exhibit a volatile elastic energy over time. The elastic energy increases gradually as granules slowly deform (as blocks deform during the interseismic phase of the earthquake cycle), and it decreases rapidly due to intermittent granule rearrangement events (due to earthquakes). Pursuing this analogy, we find that the dynamics displayed by the readings of the seismogenic plate boundary, as manifested by their velocity fluctuations, are consistent with those characterizing analogous 2D sheared deformable granular media, where the velocities $\mathbf{v}_i$ are associated with densely packed granules or bubbles constrained between two shearing plates at a low shearing rate. Namely, we show that, consistent with findings for slowly sheared granular media [17], the distribution of velocity fluctuations $P(\delta\mathbf{v})$ deviates from a Gaussian, exhibiting broad tails, and the correlation function decays as a stretched exponential. We note that the velocity profile deviates from the linear profile expected for a homogeneously sheared elastic body, ruling this out as an alternative mechanism.

This analogy, based on kinematic characteristic, allows us to make predictions concerning time scales and length scales associated with the dynamics at a seismogenic plate boundary. One of the primary observations in fault block systems is the ratio of time needed for the coseismic release of elastic strain (earthquakes) and the time it takes for slow plate motions (10–100 mm/yr) to accumulate elastic strain. Following the analogy with sheared granular systems in Ref. [17], we consider the time scales of the systems, defining τ_{up} as the average duration of the energy buildup between intermittent sharp energy releases, and τ_{dn} as the average duration of these energy drops. Ono *et al.* [17] found that the ratio of these characteristic times follows

$$\tau_{\mathrm{dn}}/\tau_{\mathrm{up}} = 7.9\dot{\gamma}^{0.4}, \tag{5}$$

where $\dot{\gamma} = \dot{\epsilon}\tau_d$ is the normalized shear rate, and τ_d is the characteristic time scale in the model, the duration of a

TABLE I. Observed and predicted [17] ratio of earthquake cycle timing τ_{dn}/τ_{up}, where τ_{dn} is the duration of an earthquake, equivalent to the time of a rearrangement event in a granular system, and τ_{up} is the time between earthquakes where the elastic strain is accumulated, equivalent to the time between rearrangement events. The predicted ratio is within the range of observed values. Also shown are observed values for the shear strain rate $\dot{\epsilon}$, the crack tip evolution τ_d, and the normalized shear strain rate $\dot{\gamma}$, substituted in Eq. (5) to yield the predicted ratio of earthquake cycle timing. See the text for further details.

Parameter	Description	Value
τ_{dn}	Duration of earthquake	10–600 s [24]
τ_{up}	Earthquake recurrence interval	10^8–$10^{11.5}$ s [24]
$\dot{\epsilon}$	Shear strain rate	10^{-15} s^{-1} [25]
τ_d	Crack tip evolution	10^{-9} s [23]
$\dot{\gamma} = \dot{\epsilon}\tau_d$	Normalized shear strain rate	8×10^{-24}
τ_{dn}/τ_{up}	Observed ratio	$6\times10^{-6}-3\times10^{-11}$
$t_{dn}^{pred}/t_{up}^{pred}$	Predicted ratio [Eq. (5)]	5×10^{-9}

rearrangement event [17,18]. For the earthquake system, τ_{dn} is the characteristic duration of an earthquake, and τ_{up} is the earthquake recurrence interval. Observed values and their ratio τ_{dn}/τ_{up} are given in Table I. The ratio is found to be consistent with the ratio predicted by Eq. (5), thus relating these time scales to the observed sheared strain rate $\dot{\epsilon}^{obs}$, and the time scale of the system τ_d, suggested to be the nanosecond value for the crack tip evolution time scale [23].

Moreover, we recall that, in slowly sheared granular material, the value of the stretched exponential fit of the spatial correlation function in Eq. (4), ξ, is associated with the average granule or bubble size [17], suggesting that the length scale associated with the seismogenic plate boundary is roughly 90 km. This value is 4–5 orders of magnitude larger than the granular fault gauge [11], indicating that plate boundaries may be treated as granular systems at a macroscopic scale, with the length scale ξ associated with the characteristic grain or bubble size, here representing the characteristic size of tectonic blocks in the southern California fault network (i.e., the average distance between faults). This inference is also consistent with the 120 km mean length scale calculated from models of kinematically distinct fault bounded blocks in southern California required to explain GPS velocities at 1.67 mm/yr resolution [26]. Independent studies of southern California [27,28] appear to have assumed similar characteristic length scales based on the assumption that geologically prominent faults determine the characteristic block length scale.

Furthermore, we show that the heavy tails of the fluctuation distributions do not depend on the form of major fault accommodating most of the deformation between the two plates—the San Andreas Fault (see the SM for details [22]). This further strengthens the concept that the macroscopic tectonic dynamics are governed by the intricate fault and block system, rather than just a single dominant major fault.

Lastly, this model provides an explanation for the clustered and intermittent fault behaviors observed in the geologic record as a response to the rapid reorganization of force chains by the earthquakes themselves. Geological observations of macroscopic fault system activity have revealed an array of behaviors, for example, at the seismically active southern California plate boundary, observations of paleo-earthquake activity range from nearly periodic [29,30] to clustered [31], and out of phase. Specific examples of oscillatory behavior, over multiple earthquake cycle time scales, include out of phase fault slip between the Los Angeles Basin and the eastern California shear zone [32], as well as between the subparallel San Andreas and San Jacinto faults [33]. These observations of diverse fault activity can be explained by a model where plate boundaries are considered as macroscopic granular shear zones near the jamming transition [23] with effective granule sizes >10 km. Granule sizes at this scale enable earthquakes themselves to redistribute forces within plate boundaries by creating and destroying force chains and producing complex time evolving fault slip rate histories.

In summary, in this Letter we pursued the analogy between 2D sheared deformable granular media and seismogenic plate boundaries. We found that, consistent with findings for slowly sheared granular media [17], the distribution of velocity fluctuations $P(\delta\mathbf{v})$ deviates from a Gaussian, exhibiting broad tails, and the correlation function decays as a stretched exponential. This analogy also allowed us to relate the ratio of two characteristic time scales, the characteristic duration of an earthquake and the earthquake recurrence interval, with the observed sheared strain rate and the nanosecond value for the crack tip evolution time scale. Moreover. we found that the characteristic length scale associated with the average bubble or grain size is roughly 90 km, here representing the characteristic size of tectonic blocks in the southern California fault network. The similarity of the statistical description between heavy-tailed grain scale experiments and plate boundary scale GPS velocity fluctuations suggests that the granular approximation may be a useful mathematical framework for understanding and exploring the latter.

The authors thank Ido Regev and Yohai Bar-Sinai for the helpful observations and fruitful conversations.

*ymeroz@seas.harvard.edu

[1] R. E. Abercrombie, J. Geophys. Res. **100**, 24015 (1995).
[2] M. Ishii, P. M. Shearer, H. Houston, and J. E. Vidale, Nature (London) **435**, 933 (2005).
[3] S. Ozawa, T. Nishimura, H. Suito, T. Kobayashi, M. Tobita, and T. Imakiire, Nature (London) **475**, 373 (2011).

[4] A. C. Lawson and H. F. Reid, Carnegie Institution of Washington Report No. 87, 1908.
[5] A. Plesch *et al.*, Bull. Seismol. Soc. Am. **97**, 1793 (2007).
[6] C. Jennings, 1975.
[7] L. M. Wallace, J. Beavan, R. McCaffrey, and D. Darby, J. Geophys. Res. **109**, B12406 (2004).
[8] D. S. Fisher, K. Dahmen, S. Ramanathan, and Y. Ben-Zion, Phys. Rev. Lett. **78**, 4885 (1997).
[9] K. Dahmen, D. Ertaş, and Y. Ben-Zion, Phys. Rev. E **58**, 1494 (1998).
[10] E. Aharonov and D. Sparks, Phys. Rev. E **60**, 6890 (1999).
[11] E. Aharonov and D. Sparks, J. Geophys. Res. **109**, B09306 (2004).
[12] Y. Bar-Sinai, R. Spatschek, E. A. Brener, and E. Bouchbinder, Phys. Rev. E **88**, 060403(R) (2013).
[13] California Department of Conservation, Division of Mines and Geology, "Fault activity map of California and adjacent areas, with locations and ages of recent volcanic eruptions," 2014.
[14] California Department of Conservation, Fault activity map of California, http://maps.conservation.ca.gov/cgs/fam/ (2010).
[15] C. Kreemer, G. Blewitt, and E. C. Klein, Geochem. Geophys. Geosyst. **15**, 3849 (2014).
[16] D. L. Anderson, *New Theory of the Earth* (Cambridge University Press, Cambridge, England, 2007).
[17] I. K. Ono, S. Tewari, S. A. Langer, and A. J. Liu, Phys. Rev. E **67**, 061503 (2003).
[18] D. J. Durian, Phys. Rev. Lett. **75**, 4780 (1995).
[19] D. J. Durian, Phys. Rev. E **55**, 1739 (1997).
[20] J. Lauridsen, M. Twardos, and M. Dennin, Phys. Rev. Lett. **89**, 098303 (2002).
[21] A. Rahman, Phys. Rev. **136**, A405 (1964).
[22] See Supplemental Material at http://link.aps.org/supplemental/10.1103/PhysRevLett.119.138501 for a demonstration of independence of results on Fault geometry or noisy statistics, showing that substantial fluctuations are exhibited in an area of ∼100 km across the fault, and showing that the value of ξ is robust.
[23] Y. Ben-Zion, Rev. Geophys. **46**, RG4006 (2008).
[24] C. H. Scholz, *The Mechanics of Earthquakes and Faulting* (Cambridge University Press, Cambridge, England, 2002).
[25] Z.-K. Shen, D. D. Jackson, and Y. Y. Kagan, Seismol. Res. Lett. **78**, 116 (2007).
[26] J. P. Loveless and B. J. Meade, Geology **39**, 1035 (2011).
[27] R. McCaffrey, J. Geophys. Res. **110**, B07401 (2005).
[28] T. W. Becker, J. L. Hardebeck, and G. Anderson, Geophys. J. Int. **160**, 634 (2005).
[29] T. Fumal, R. Weldon, G. Biasi, T. Dawson, G. Seitz, W. Frost, and D. Schwartz, Bull. Seismol. Soc. Am. **92**, 2726 (2002).
[30] K. M. Scharer, R. J. Weldon, T. E. Fumal, and G. P. Biasi, Bull. Seismol. Soc. Am. **97**, 1054 (2007).
[31] L. B. Grant and K. Sieh, J. Geophys. Res. **99**, 6819 (1994).
[32] J. F. Dolan, D. D. Bowman, and C. G. Sammis, Geology **35**, 855 (2007).
[33] R. A. Bennett, A. M. Friedrich, and K. P. Furlong, Geology **32**, 961 (2004).